Modeling The Growth of Electronic Materials

Grant No. N00014-93-1-1105

Final Technical Report Submitted to

OFFICE OF NAVAL RESEARCH

Ballston Tower One
800 North Quincy Street
Arlington, VA 22217-5660

Submitted by

An-Ban Chen
Department of Physics
Auburn University
AL 36849

December, 1994

I. Introduction

Through the DEPSCoR program, this grant (N00014-93-1-1105) allowed Auburn University to acquire a dedicated workstation to simulate properties of semiconductors and their alloys. We have acquired a HP9000/735 workstation (named SOLID) with a sufficient speed, memory, storage, and graphic capability to perform realistic simulations. The biggest advantage of having this machine is that we are not constrained by the turn-around and CPU time imposed by a general-purpose supercomputer. Since the installation of this machine in January 1994, we have made progress in several directions. These include (1) obtaining criteria for convergence in molecular-dynamic (MD) simulations of disordered zincblende alloys, (2) obtaining accurate information about bond lengths and excess energies of disordered zincblende alloys, (3) achieving a reliable method for obtaining bulk alloy free energies and phase diagrams from finite-size Monte-Carlo (MC) simulations, and (4) establishing an effective iterative method for calculating the density matrix in an order-N algorithm. In the last step we have demonstrated the validity of the density matrix approach. Using this method, we do not need to diagonalize the one electron Hamiltonian. Thus the computing time is reduced from the N^3 to N, where N is the number of atoms per unit cell used in the simulation. These studies have demonstrated the ability of SOLID for performing realistic MD and MC simulations. These results are being used to investigate a new class of III-V infrared materials and the wide-gap semiconductors SiC, GaN, AlN and their alloys.

II. Convergence of Structural Properties and Energies in Pseudo-binary Alloys

To start our molecular-dynamics simulation of disordered zincblende alloys, we used a simple classical potential, the valence force field model (VFF). In VFF the excess energy of an alloy is given by

$$\Delta E = \frac{3\alpha}{8d^2}\sum_i [\Delta(\vec{r}_i \cdot \vec{r}_i)]^2 + \frac{3\beta}{8d^2}\sum_{i>j} [\Delta(\vec{r}_i \cdot \vec{r}_j)]^2, \qquad (1)$$

where the first term sums over all the bonds and the second term sums over all pairs of bonds sharing a common atom. $\Delta(\vec{r}_i \cdot \vec{r}_i)$ is the deviation of square of the bond length and d is the average bond length of the alloy. Similarly $\Delta(\vec{r}_i \cdot \vec{r}_j)$ is the deviation of the dot product of the two bond vectors from $d_i d_j \cos\theta$, where θ is the angle between two tetrahedral bonds with $\cos\theta = -1/3$. The bond stretching force constant α and the bond angle restoring force β take the pure-crystal values when the bonds involved can be identified as such. Otherwise, the mean values are used. For example, in $Ga_{1-x}In_xAs$ if both bonds are Ga-As bonds, then the β value is that of GaAs. If the pair involves a Ga-As bond and an In-As bond, then the mean value is used. The values of α and β for the constituent compounds have been determined previously [1].

In the MD simulation, we use the periodic supercell approach. First we decide the number of atoms N per unit cell to be simulated. The values of N studied range from 64 to 1000. For a given N and a given concentration x (here we only consider x=0.25, 0.5

and 0.75), random numbers are generated and used to place the atoms on the virtual crystal (average) positions. These atoms then follow the Newton's equation of motion with forces computed as the negative of the gradients of ΔE with respect to the atomic positions. To find the equilibrium positions, dynamic frictional forces are introduced. The calculation is stopped when no appreciable motion for all atoms is reached. The excess energies and the detailed structural information such as the average values and rms widths of first and the second bond lengths and the bond angles are obtained for each configuration (the initial assignment of site occupations). The variations of these quantities with different configurations are then studied.

It should be mentioned that MD is not the most efficient way to study the static properties such as the present case. For example, the steepest descend and conjugate gradient methods are faster. However, we want to initiate a MD calculation and calibrate its speed and accuracy. The techniques developed here can be employed later to study dynamic processes.

Fig. 1 shows the average bond lengths of the first neighbor InAs bonds in $Ga_{1x}In_xAs$ at x=0.5 for different configurations using N=64. It shows fluctuations with a maximum deviation of 0.014A. Fig. 2 shows the same plot with a larger N=216. With this N the maximum deviation is reduced to 0.008 A. Finally, in Fig. 3 for N=512, the maximum deviation is further reduced to 0.004 A. These results show that the average values of bond lengths can either be obtained from a small N but averaged over a large number of configuration, or form a single calculation with a large N.

Fig. 4 shows the excess energies per pair of atoms ΔE calculated for N=64. Compared with the bond lengths, ΔE has a much larger percentage fluctuation, because ΔE itself is a small. The values of ΔE averaged over the configurations is 52 meV per pair of atoms with a maximum deviation of 10 meV. Similar to the bond length, increase in N reduces the fluctuation in ΔE. As shown in Fig.6 for the case N=512, the maximum deviation in ΔE is reduced to 2 meV whereas the average value of ΔE is still 52 meV.

Detailed information about various bond angles and second-neighbor bond lengths has also been obtained for a number of systems. These results will be compared with the TB calculations and experiments in Section III. The most important message from the present calculations is that the structural properties of a random zincblende alloy can be obtained from a reasonably small N and a dozen or so of configurations, which is still faster than using a large N.

III. Tight-Binding Calculations

Calculation of the structural properties of disordered alloys using quantum theory inherently encounters a major difficulty arising from the lack of crystal translational symmetry in these systems. There are approximate theories such as the coherent-potential approximation (CPA) [2] and special quasi-random systems (SQS) [3]. CPA is useful for treating disorder potentials that are short-ranged in the coordinate space. Its ability to treat long range strain energy and associated atomic relaxation has yet to be established. SQS is a method that mimics a random alloy by using a crystal with a small number of atoms per unit cell. As shown in Figs. 1 through 4, the fluctuations among different configurations are quite large even with 64 atoms per unit cell. Picking a particular crystal with a smaller number of atoms per unit cell to represent a random alloy may be valid for some properties, but not for all. As was shown in Section II, with 64 atoms per unit, the bond length fluctuations are more tolerable than those in the excess energies. Reliable results can only be obtained by averaging over a number of configurations.

We have obtained a set of TB Hamiltonians for a collection of III-V and II-VI compounds from our previous work [1]. These Hamiltonians, besides being able to reproduce the experimental quantities such as bonding energies, bulk moduli B, and the shear coefficients C_{11}-C_{12} , are also capable of producing accurate values for other physical properties not used in the fitting, e.g., the shear coefficients C_{44}, the transverse optical phonon frequencies, and the Kleinman internal relaxation parameters. These Hamiltonians can compete favorably against any other Hamiltonian, empirical or *ab-initio*, for an accurate calculation of structural properties of zincblende alloys. They have been used to calculate the excess energies and the bond lengths of a number of long-range ordered semiconductor alloys [4]. Our results, along with the best *ab-initio* calculations, have firmly established that these long-range alloys are not thermally stable bulk states at the growth temperatures. The origin of ordering in semiconductor alloys found from epitaxial growth must be due to surface bonding and growth kinetics.

Using SOLID, we have carried out TB calculations for a number of disordered zincblende alloys using N=64 per unit cell. The Hamiltonian is a 256x256 matrix for a given k-point. It is diagonalized directly in each relaxation step. Four special k points were used to evaluate the valence electron band energies. However, we do not need to start with the virtual-crystal positions. The final positions determined from the VFF calculation can be used as the first step in the TB calculation. Also, instead of doing MD, the steepest descend method is used. Doing so makes the TB calculation manageable. We are assembling these results for publication. Below we show the results for a typical alloy.

In Figs. 7 and 8, the calculated average bond lengths between the first neighbor atoms in $Ga_{1-x}In_xAs$ are compared with the straight line fitted to the data obtained from the EXAFS experiment [5]. While both the theory and experiment show the bimodal bond length distribution first discovered by Miklesen and Boyce [5], there are quantitative differences. Both TB and VFF results show a detectable departure from the

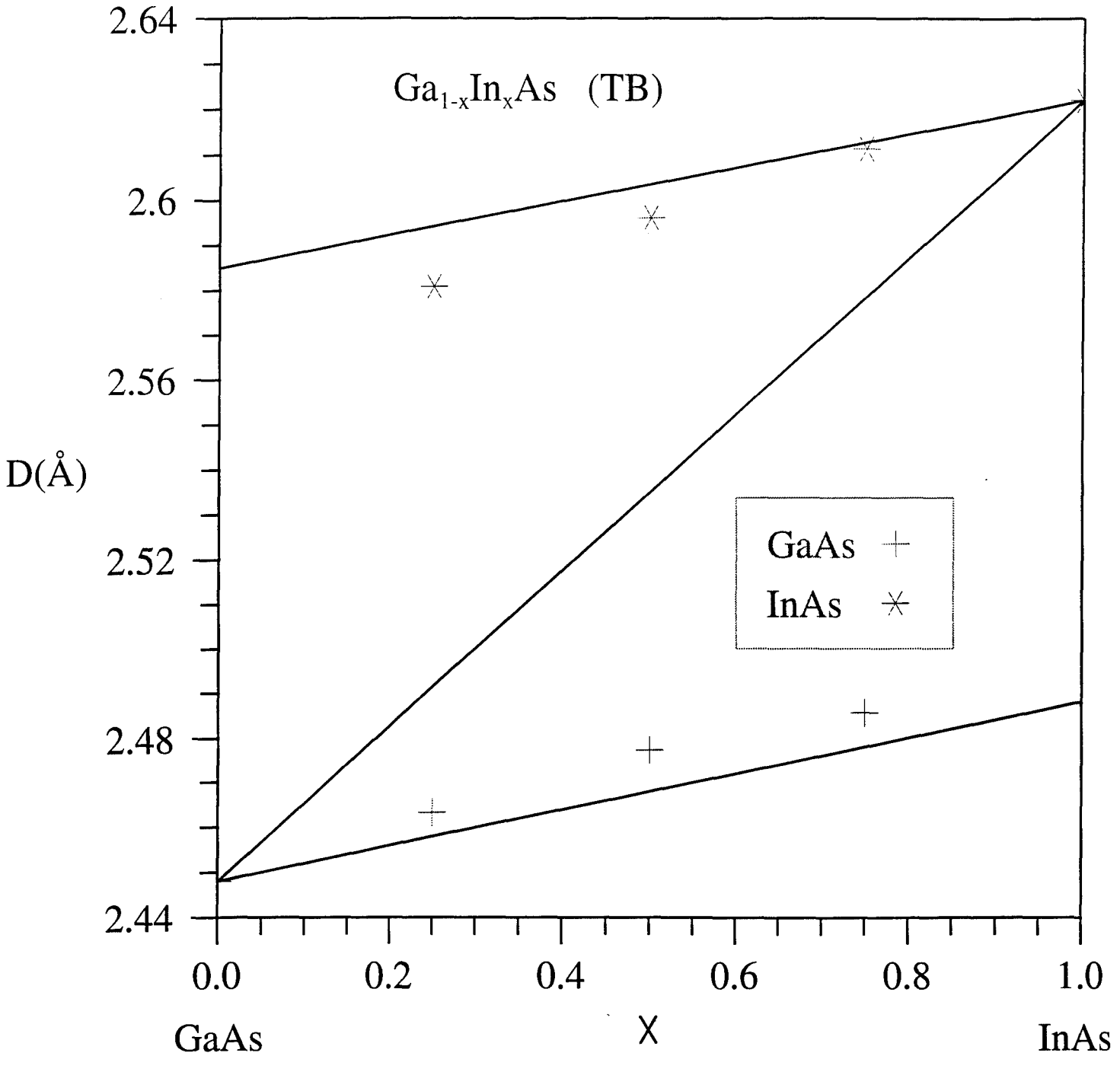

Fig.7 Plot showing how 1st neighbor bond lengths of GaInAs depend on concentration.

linearity at he 'impurity' limit, i.e., In-As bonds at small x tend to bend toward smaller values and Ga-As bonds at x≈1.0 also tend to bend toward smaller values. This skewed trend can be attributed to the fact that GaAs has larger elastic constants than InAs. Fig. 9 shows the second-neighbor As-As distances. Again these results show a bimodal distribution. However, while the experimental in results [5] give the two bond lengths nearly equal to their respective values in the pure constituent compounds, the calculated values show a detectable x dependence. Fig. 10 shows the second-neighbor distances for the Ga-Ga, Ga-In, and In-In pairs. Although Ga-Ga distance is slightly shorter than the In-In distance, their values are closer to the average value than to their respective values in the constituent compounds. The Ga-In distance is well described by the average value of the constituents. These calculated values are in excellent agreement with the experimental results [5]. While EXAFS enables to measure the bond lengths with an acceptable precision for the first and second neighbors, it can not measure the bond angles directly. An accurate simulation can provide all the information needed. Table 1 lists the average bond angles for Ga-As-GA, Ga-As-In, In-As-In, As-Ga-As and As-In-As and their rms fluctuations. It is interesting to see that the averaged angles between two bonds joining at Ga or In maintain the perfect crystal value $\cos\theta=-1/3$, with $\theta=109.5^{\circ}$. These results combined give a rather complete picture of the local atomic positions in a disordered zincblende alloy.

Table 1. Average bond angles (in degrees) in $Ga_{1-x}In_xAs$. The numbers in the parentheses are the rms deviations

x	0.25	0.5	0.75
Ga-As-Ga	110.4 (1.7)	111.6 (1.9)	112.1 (1.6)
Ga-As-In	108.5 (1.6)	109.4 (1.8)	110.8(1.5)
In-As-In	105.7(1.2)	107.3 (1.8)	108.2 (1.7)
As-Ga-As	109.5 (1.7)	109.5 (2.0)	10.9.5 (1.4)
As-In-As	109.5(1.9)	109.5 (2.0)	109.5 (1.8)

Fig. 11 is a plot of the excess energy per pair of atoms at three concentrations. These values show a noticeable deviation from the regular-solution form $\Delta E=x(1-x)\Omega$. The ΔE value for the 50-50 alloy, when compared with those in the long-range ordered alloys [4], is very close to the value in the CuAuI structure. However, the first-neighbor bond lengths are closer to the those in the Chalcopyrite structure. When combined with Monte-Carlo simulations, the temperature-dependence of these quantities can be investigated. The T-dependent excess energies can be used to derive Helmholtz free energies and phase diagrams for alloys.

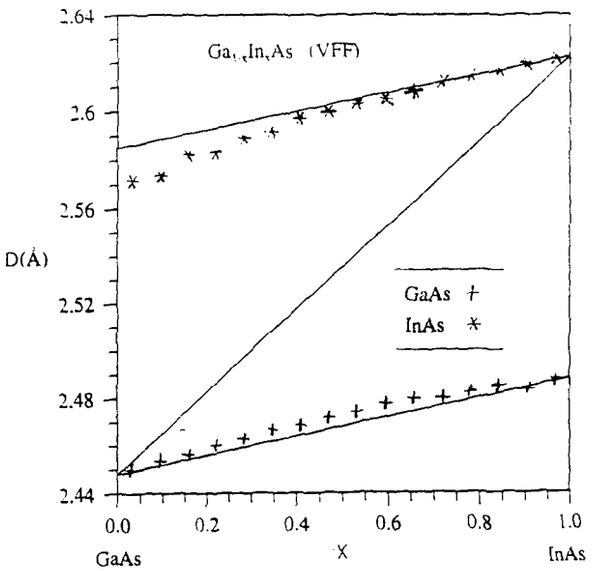

Fig.8 Plot showing how 1st neighbor bond lengths of GaInAs depend on concentration.

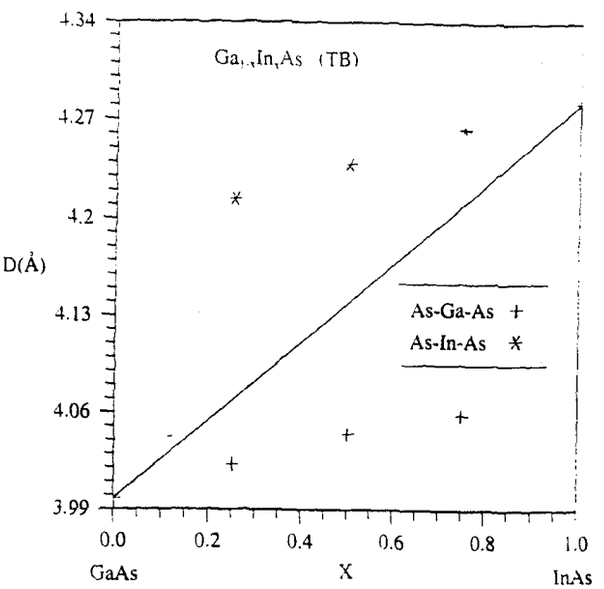

Fig.9 Plot showing 2nd Neighbor cation-cation bond lengths of GaInAs for various concentrations.

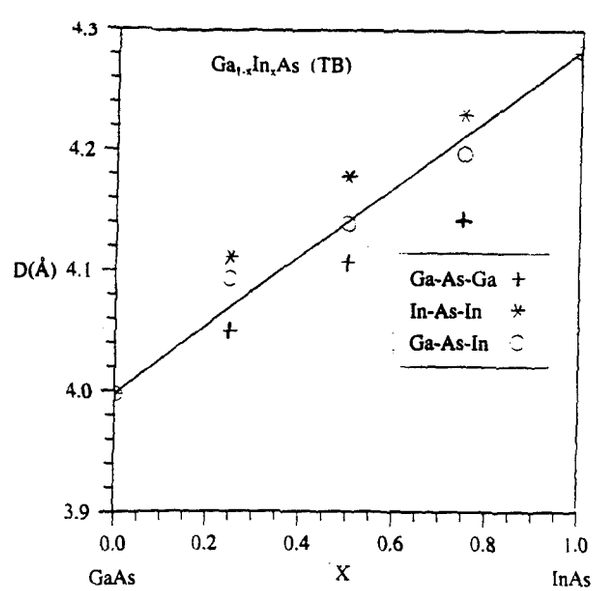

Fig.10 Plot showing 2nd Neighbor anion-anion bond lengths of GaInAs for various concentrations.

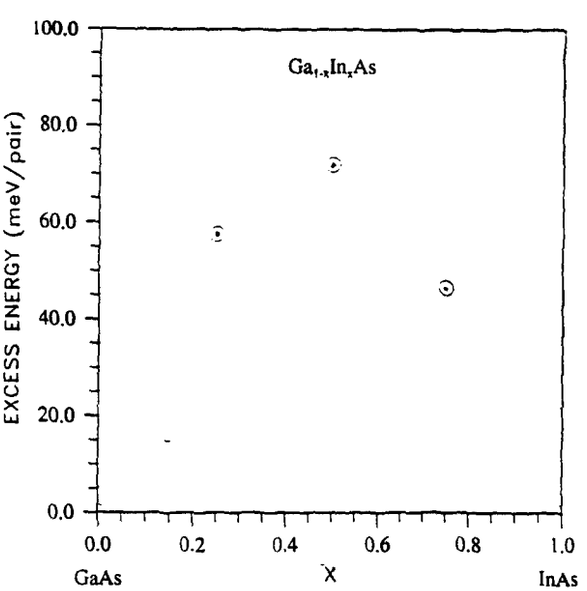

Fig.11 Plot showing Excess Energy of GaInAs for at 25% , 50 % and 75% concentration.

IV. Monte Carlo Simulations

There are three major issues in Monte-Carlo (MC) simulations of phase diagrams at the atomic scale: (1) accurate Hamiltonian, (2) computational speed, and (3) extrapolation from finite-size to bulk. For zincblende semiconductor alloys, the TB Hamiltonians described in Section III are believed to be accurate for the solid states. Thus for the calculation of the solid solution free energies and the phase diagrams we still have two problems to solve. In this period, we have established a MC procedure and have done a detailed study for the finite-size problem. We focus on the two-dimensional Ising model. Our objective is to use as little information as possible about the scaling rules to deduce accurate bulk free energies directly from finite-size MC simulations.

To simulate alloy with a fixed concentration, we fix the magnetic moment in the Ising model. For a square lattice, we have simulated systems with N=100, 256, 400, 676 and 900. For a given N and x, the xN up spins are placed in a given lattice randomly. Then the sites of these xN up spins are exchanged with those of the (1-x)N down spins through random exchanges. The average energy $\Delta E(\beta)$ at a given temperature T=1/(kβ) is calculated as an average over ensembles of all states in the exchange cycles governed by a Markovian process. Converged energies are found for all cases less than 20000 cycles per atom are completed. The Helmholtz free energy at a given β is then calculated from

$$\beta\Delta F = -S(0) + \int_0^{\beta} \Delta E(\beta) d\beta \,, \qquad (2)$$

where S(0) is the entropy of a random alloy (at β=0). Once ΔF(x,T) is available for all x and T, the miscibility gap for a given T can be obtained from the condition $\partial F/\partial x = 0$, because ΔF in the present case is an even function about x=0.5.

It is interesting to see the equilibrium states produced in our MC simulations. At high T we expect that the system remains a disordered state after a long cycle of simulations, whereas we expect phase separation at low T. All energies and kT in this section are scaled by the effective pair energy J such that ε_{AB}=J, ε_{AA} =ε_{AA}=0. Fig.12 shows the case for N=1600 with x=0.5 at high T. The distribution maintains disordered even after 20000 cycles per atom of exchanges are completed. Figs. 13 and 14 show the populations of the same system at a temperature below the critical temperature T_c =2.26 for the present case. The two figures correspond to the results after 3500 and 20000 exchanges per spin are completed respectively. They clearly show phase separations. The longer time the simulation goes the more complete domains we obtain.

Fig. 15 shows the plots of excess energies as a function of temperature T for x=0.5. These plots include the exact values and the values from our MC simulations with N=100, 256, 400, 676 and 900. These plots show that at high $T>T_c$ the energies from finite-size simulations are already accurate. As T approaches T_c the deviations become larger. At $T<T_c$ the deviation is as large as the energy itself. Since the size dependence

Fig. 12 A snapshot of the atomic postions of a 50-50 binary alloy at $T=4.4T_c$ after 20000 cycles exchanges per atom are performed.

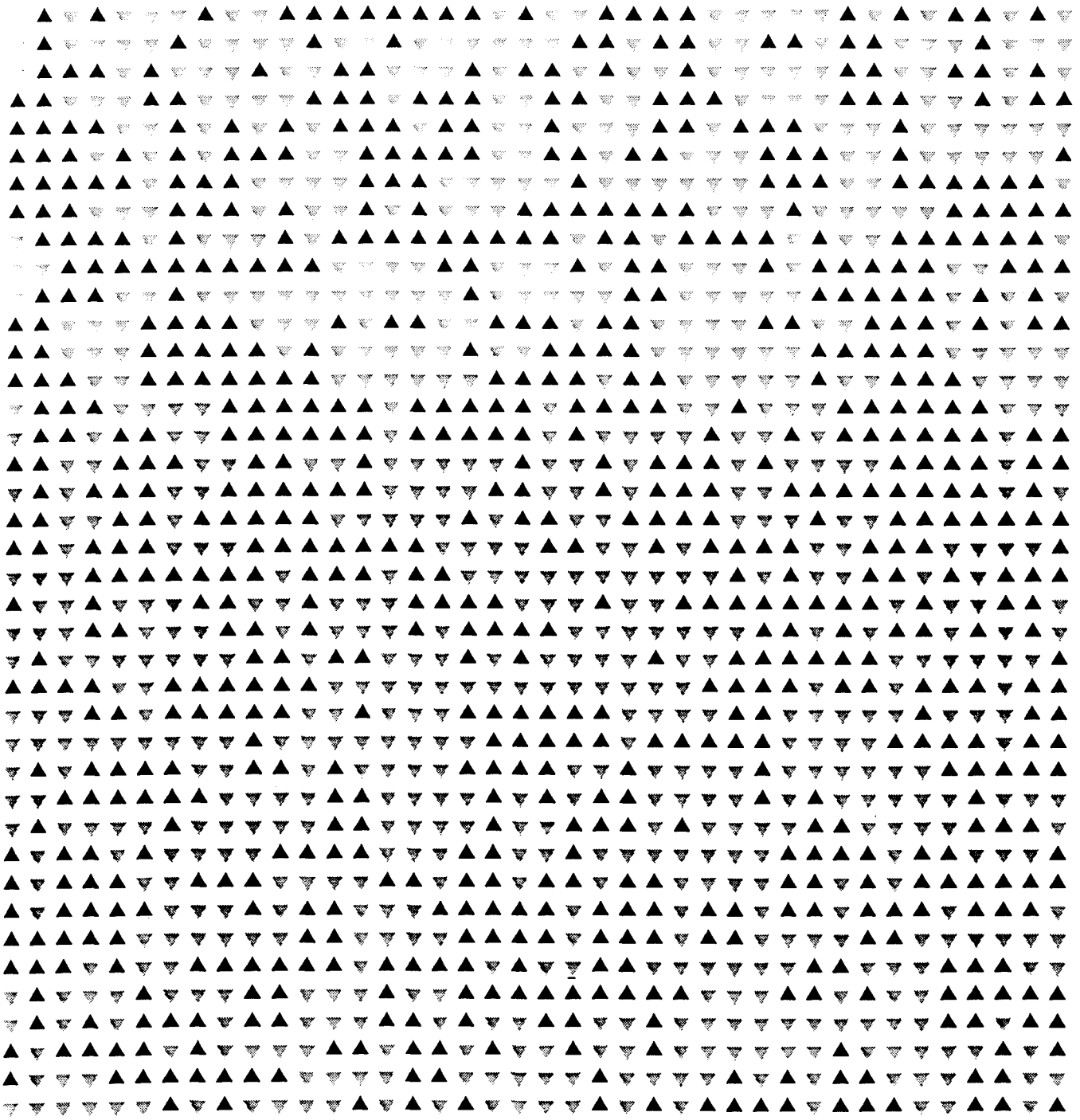

Fig. 13 A snapshot of the atomic postions of a 50-50 binary alloy at $T=0.885T_c$ after 3500 cycles exchanges per atom are performed.

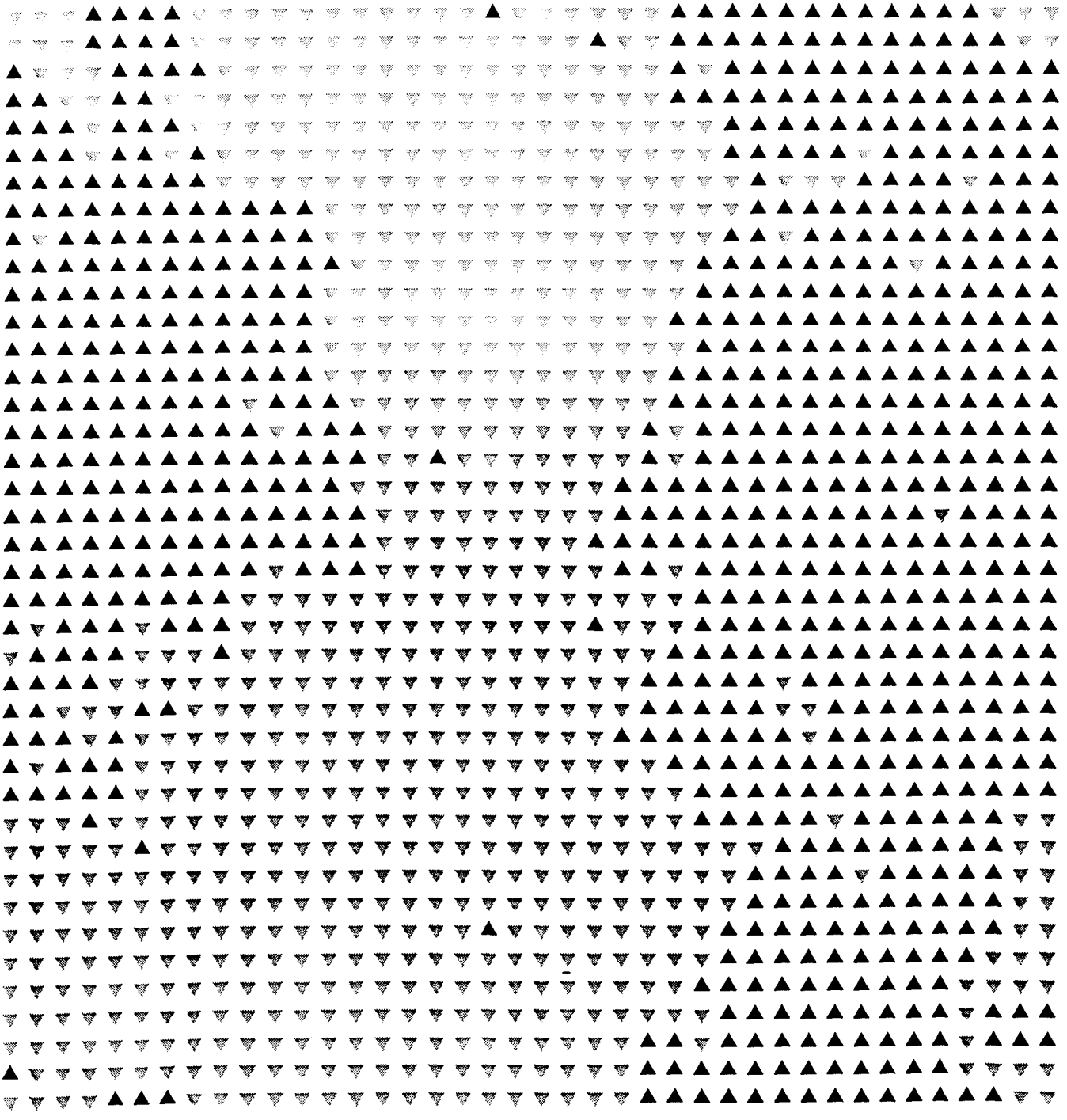

Fig. 14 A snapshot of the atomic postions of a 50-50 binary alloy at $T=0.885T_c$ after 20000 cycles exchanges per atom are performed.

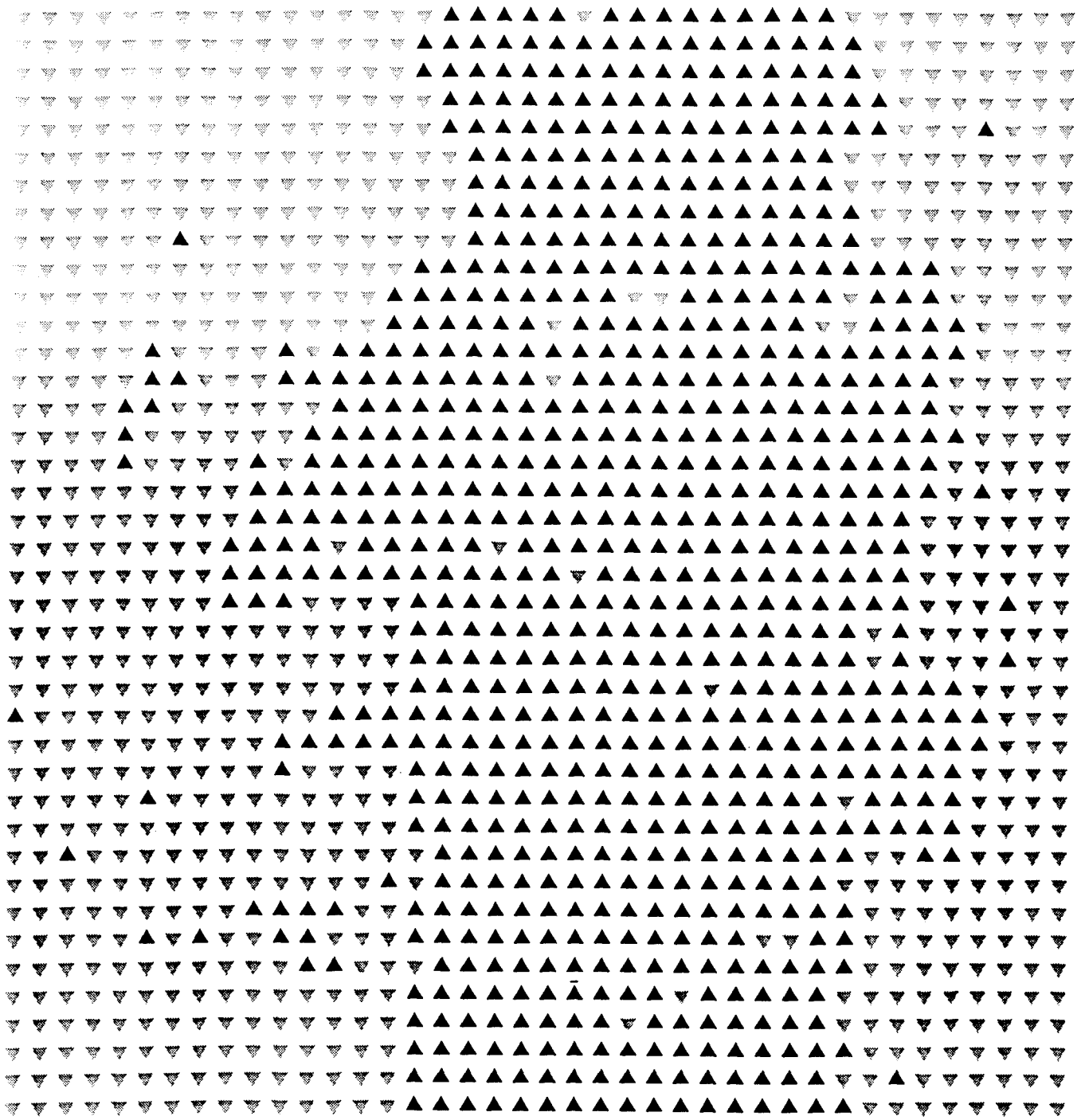

of ΔE varies as T varies from above to below T_c, and the dependence for the small range of N in our simulation may not apply to the bulk limit, we have tried the following simple form to extrapolate the bulk energy ΔE_B:

$$\Delta E_B = \Delta E_N - A / N^{\alpha}, \qquad (3)$$

where α and A are obtained from a least square fit of this equation to several calculated values ΔE_N. The α values thus obtained are further fitted to a simple function of temperature. Doing so we are able to obtained ΔE_B as a smooth function of T for a given x. These ΔE_B are then used to calculate ΔF_B according to Eq.(2). Finally ΔF_B are interpolated to generate the entire function of x and T. In Fig. 16, the extrapolated ΔE values for x=0.5 are compared with the Onsager's exact results. This comparison shows that our procedure yields accurate ΔE for $T>T_c$, generates adequate results for $T\approx T_c$, and gives only rough estimate for $T<T_c$. Similar conclusion can also be drawn for the free energy ΔF as shown in Fig. 17. These results tell us that we should utilize the high-temperature data whenever possible.

Figure 18 displays ΔF as a function of x for several T values for the case with N=400. From these curves, we evaluate $\partial F/\partial x$ as a function of x as x increases from 0. The miscibility gap is determined from the condition $\partial F/\partial x=0$ at the smallest x value. Fig. 19 shows a similar family of curves for the extrapolated bulk ΔF. Note that the curves flatten out for T less than T_c as they should. From this point of view, the extrapolated curves are more accurate than the finite-size results as far as representing the bulk properties. The calculated miscibility curves are displayed in Fig. 20. These include the exact curve, the curve based on the extrapolation and those of several finite-size systems. These results show that the simple extrapolation procedure used her is a reasonable way to obtain bulk free energies and phase diagrams.

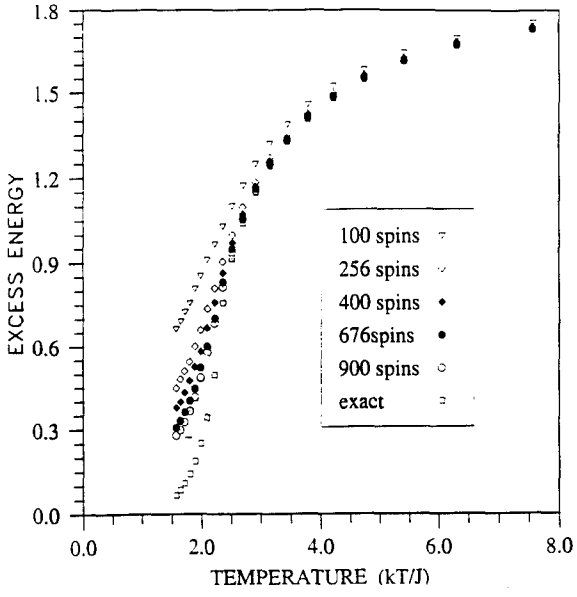

Fig.15 Energy Curves for binary alloy of different sizes.

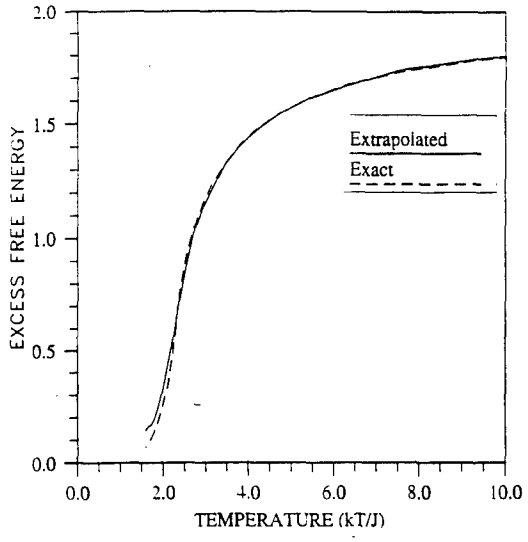

Fig.16 Comparison of Excess Energy for binary alloy at 50% concentration and Onsager's exact solution to ising model.

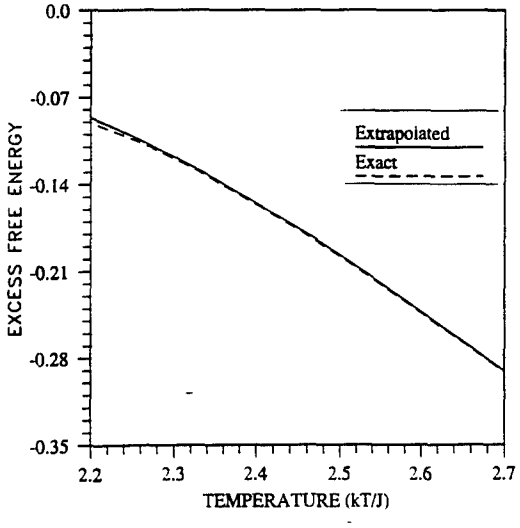

Fig.17 Comparison of Energy for binary alloy at 50% concentration and Onsager's exact solution to ising model.

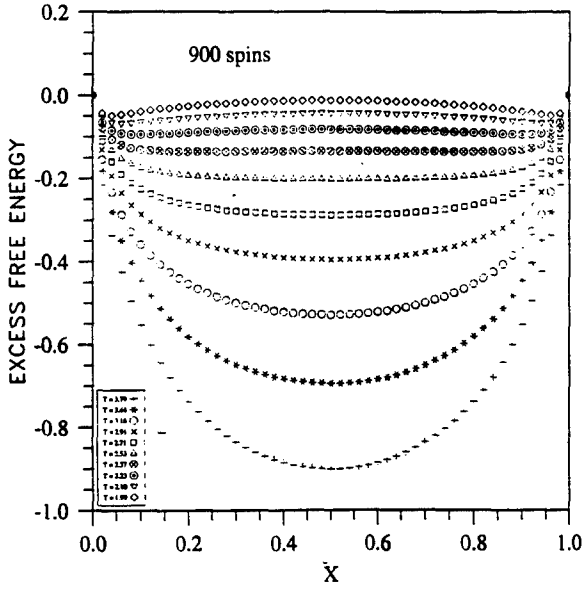

Fig.18 Free Energy Curves for binary alloy of 900 spins for several temperatures.

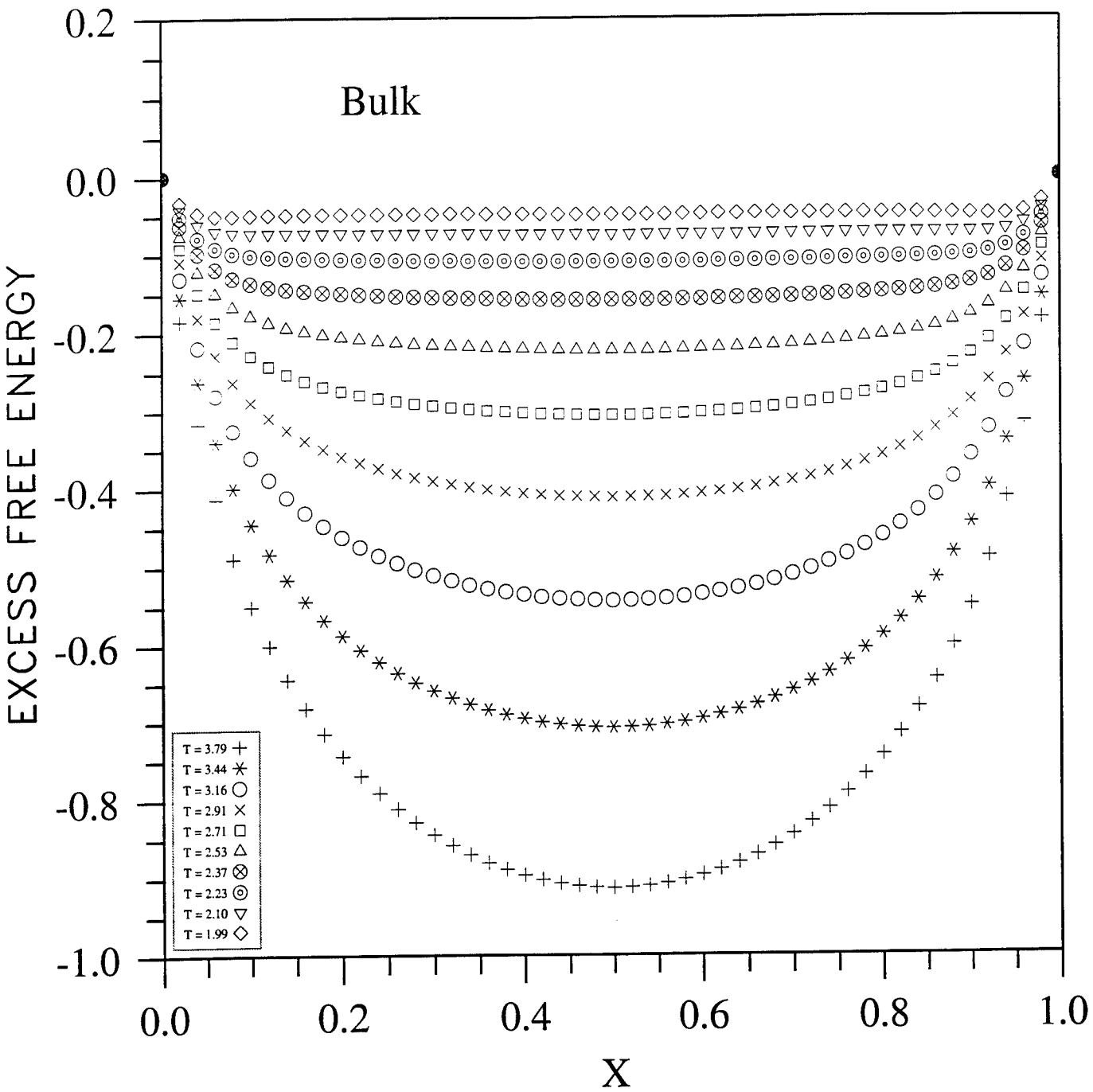

Fig.19 Extrapolated Free Energy Curves for binary alloy

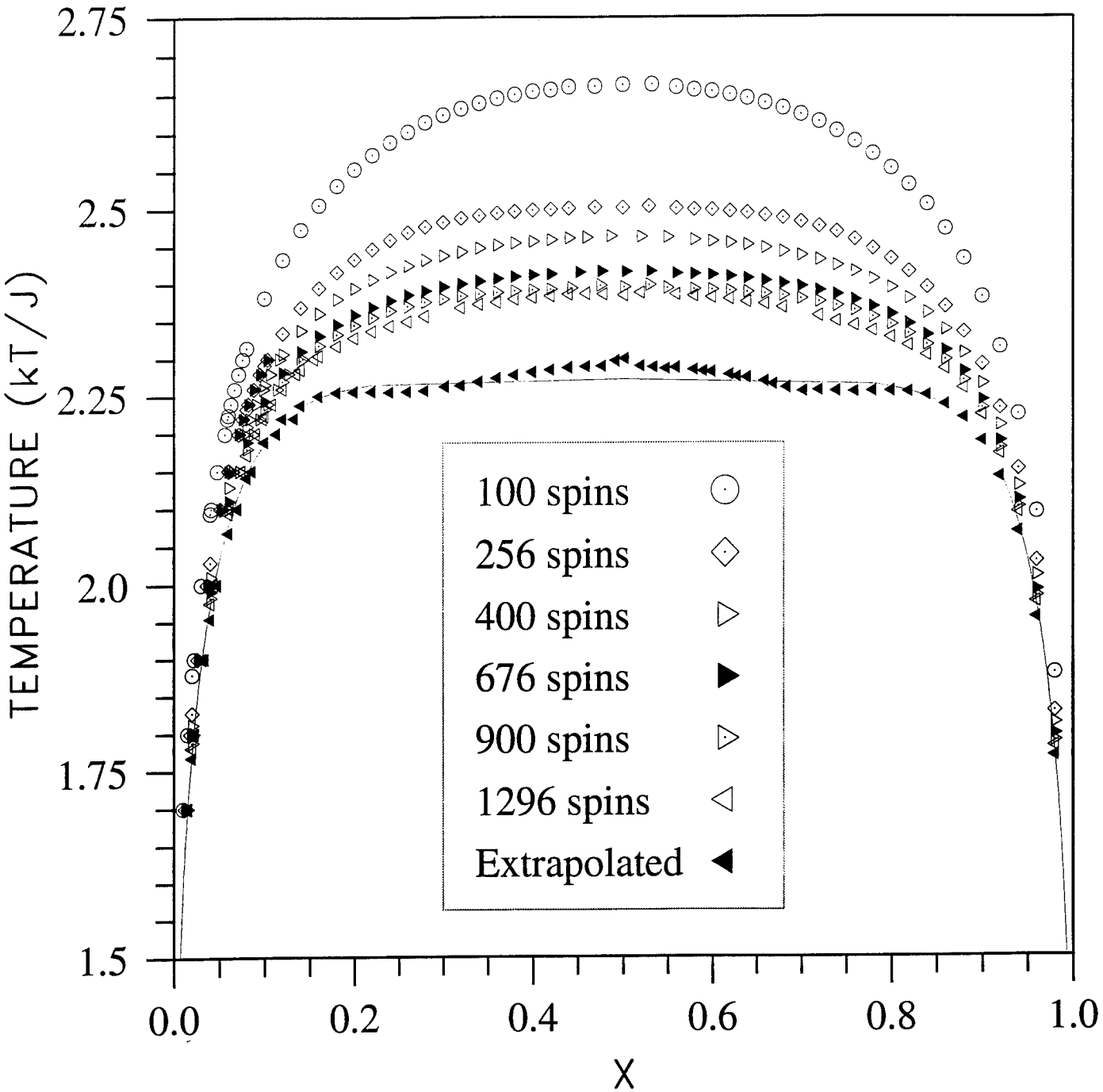

Fig. 20 Miscibility Gap obtained from free energy curves for various size systems including extrapolated {bulk}. The solid line corresponds to Onsager's exact solution

V. Density Matrix and Order-N Algorithm

Although the current LDA techniques allow calculations to be formed for a modest size with N≈100, most practical materials problems required larger calculations with N at least one or two orders larger than the current limit. The limiting factor in the current calculation is the diagonalization of the one-electron Hamiltonian H in a solid, which requires CPU time scaled as N^3. A new algorithm based on the density matrix [6] may bring about a revolution in first-principles materials simulations.

The density matrix is a projection operator onto the occupied states of H, i.e., $\rho(\mu)=\sum\theta(\mu-\varepsilon_n)$, where μ is the chemical potential (Fermi level), ε_n are the eigen values of H, and $\theta(x)=1$ for $x\geq 0$ and $\theta(x)=0$ for $x<0$. Once we know ρ, we can compute all the essential quantities. For example, the density of states is given by $D(E)=d\rho(E)/dE$, the electronic density is given by $n(\vec{r}) =< \vec{r}|\rho|\vec{r} >$, and the total band-structure energy is given by $E_{el}=Tr(\rho H)$. One can imagine that, if ρ is obtainable from multiplication of short-ranged matrices, then the calculation is scaled linearly with N. This is the order-N algorithm.

We have devised a simple and effective iterative method for ρ. We have tested this procedure in several tight-binding models and have confirmed the validity of this method. For example in Table 2, we show the total electronic energies per unit cell in the first few iterations for ρ before the minimum energy is reached. The model used is a first-neighbor sp TB Hamiltonian for GaAs. In the first row, ρ is truncated at the first neighbors, and in the second column it is truncated at the second neighbors. This table shows that the reasonably accurate band structure energy can be obtained from a short-ranged density matrix in several iterations.

Table 2. Total electronic energies (in eV) per unit cell calculated from density matrix in the first few iterations. The first and the second rows correspond to density matrices that are truncated at the first and second neighbors respectively.

							exact
1st	-21.637	-26.531	-29.916	-29.713	-30.011	-30.021	-31.396
2nd	-21.637	-26.530	-30.317	-30.721	-31.042	-31.093	

Conclusion

Realistic Molecular-dynamics and Monte-Carlo simulation of materials at the atomic and molecular level is the future of materials modeling. The computer SOLID funded by this grant has given us an opportunity to explore this possibility. In one year we have performed calculations to study several key issues concerning accurate Hamiltonian, computational speed, and extrapolation from finite size to real system. Our TB Hamiltonians are accurate enough for the structural properties of common zincblende alloys. SOLID has generated all the calculations reported here. We want to extend the calculations to the liquid states and expand our systems to include new III-V infrared alloys such $In_{1-x}Tl_xP$ and $In_{1-x}Tl_xAs$ and wide-gap semiconductors. For these studies very little experimental information is available, so we need to utilize the *ab-initio* LDA more effectively. A simple approach is to use LDA as a bench mark to deduced the TB Hamiltonian from order structures. However, with the new order-N algorithm, it is not unrealistic to think about using LDA directly in the simulating. We will take full advantage of SOLID to explore this new front.

References

1. A.-B Chen, A. Sher and W.T. Yost, Chapter 1 in **Mechanical Properties of Semiconductors**, Semiconductor and Semimetal Vol 37 (Academic Press, 1992).

2. K. Hass, B. Velicky, and H. Ehrenreich, Phys. Rev. B29, 3697, 1984; A.-B. Chen and A. Sher, J. Vac. Sci. Technol. 21(1), 138 (1982).

3. S.-H. Wei, L.G. Ferreira, J.E. Bernard, and A. Zunger, Phys. Rev. B42, 9622 (1990).

4. C.-Y. Yeh, A.-B. Chen, and A. Sher, Phys. Rev. B43, 9138 (1991).

5. J.C. Mikklesen, Jr. and J.B. Boyce, Phys. Rev. B28, 7130 (1983).

6. M. Daw, Phys. Rev. B47, 10895 (1993); X.-P. Li, R.W. Nuns, and D. Vanderbilt, Phys Rev. B47, 10891 (1993).